REPORT DOCUMENTATION PAGE

Form Approved
OMB No. 0704-0188

1. REPORT DATE *(DD-MM-YYYY)*	2. REPORT TYPE	3. DATES COVERED *(From - To)*
11-12-2008	Journal Article	

4. TITLE AND SUBTITLE

Non-Porous Organic Solids Capable of Dynamically Resolving Mixtures of Diiodoperfluoroalkanes (Postprint)

5a. CONTRACT NUMBER

5b. GRANT NUMBER

5c. PROGRAM ELEMENT NUMBER

6. AUTHOR(S)
P. Metrangolo, Y. Carcenac, & G. Resnati (Politecnico di Milano Univ., Italy); M. Lahtinen & K. Rissanen (Univ. of Jyväskylä, Finland); T. Pilati (Univ. of Milan); A. Vij (AFRL/RZSP)

5d. PROJECT NUMBER

5e. TASK NUMBER

5f. WORK UNIT NUMBER
50260541

7. PERFORMING ORGANIZATION NAME(S) AND ADDRESS(ES)

Air Force Research Laboratory (AFMC)
AFRL/RZSP
10 E. Saturn Blvd.
Edwards AFB CA 93524-7680

8. PERFORMING ORGANIZATION REPORT NUMBER

AFRL-RZ-ED-JA-2008-596

9. SPONSORING / MONITORING AGENCY NAME(S) AND ADDRESS(ES)

Air Force Research Laboratory (AFMC)
AFRL/RZS
5 Pollux Drive
Edwards AFB CA 93524-7048

10. SPONSOR/MONITOR'S ACRONYM(S)

11. SPONSOR/MONITOR'S NUMBER(S)
AFRL-RZ-ED-JA-2008-596

12. DISTRIBUTION / AVAILABILITY STATEMENT

Approved for public release; distribution unlimited (PA #09007).

13. SUPPLEMENTARY NOTES
As published in Science 323, 1461, (2009).

14. ABSTRACT

A well-known class of organic non-porous compounds, polymethylene bismethonium iodides, undergoes selective capture and release of a,w-diiodoperfluoroalkanes in a dynamic and controlled manner, in solution and from the gas phase. Despite a lack of porosity of the starting materials, guest transport through the solid occurs readily until a thermodynamically stable porous structure is achieved, which is highly selective only to the convenient diiodoperfluoroalkane. The size matching between the inter-charge distance in the cation and the charge separation in the halogen-bonded I-···I(CF2)mI···I- superanion drives the selectivity of the process, which identifies the target diiodoperfluoroalkane even from complex industrial mixtures. The full reversibility of the process where diiodoperfluoroalkanes can first be selectively complexed and then quantitatively evacuated, yields pure fluorinated telomers and reusable decamethonium congeners.

15. SUBJECT TERMS

16. SECURITY CLASSIFICATION OF:			17. LIMITATION OF ABSTRACT	18. NUMBER OF PAGES	19a. NAME OF RESPONSIBLE PERSON
					Dr. Ashwani Vij
a. REPORT	b. ABSTRACT	c. THIS PAGE	SAR	6	19b. TELEPHONE NUMBER *(include area code)*
Unclassified	**Unclassified**	**Unclassified**			N/A

Nonporous Organic Solids Capable of Dynamically Resolving Mixtures of Diiodoperfluoroalkanes

Pierangelo Metrangolo, *et al.*

Science **323**, 1461 (2009);
DOI: 10.1126/science.1168679

Nonporous Organic Solids Capable of Dynamically Resolving Mixtures of Diiodoperfluoroalkanes

Pierangelo Metrangolo,[1]* Yvan Carcenac,[1] Manu Lahtinen,[2] Tullio Pilati,[3] Kari Rissanen,[4] Ashwani Vij,[5] Giuseppe Resnati[1,3]

Halogen bonding has increasingly facilitated the assembly of diverse host-guest solids. Here, we show that a well-known class of organic salts, bis(trimethylammonium) alkane diiodides, can reversibly encapsulate α,ω-diiodoperfluoroalkanes (DIPFAs) through intermolecular interactions between the host's I^- anions and the guest's terminal iodine substituents. The process is highly selective for the fluorocarbon that forms an $I^-\cdots I(CF_2)_mI\cdots I^-$ superanion that is matched in length to the chosen dication. DIPFAs that are 2 to 12 carbons in length (common industrial intermediates) can thereby be isolated from mixtures by means of crystallization from solution upon addition of the dissolved size-matched ionic salt. The solid-state salts can also selectively capture the DIPFAs from the vapor phase, yielding the same product formed from solution despite a lack of porosity of the starting lattice structure. Heating liberates the DIPFAs and regenerates the original salt lattice, highlighting the practical potential for the system in separation applications.

α,ω-Diiodoperfluoroalkanes (α,ω-DIPFAs) are key intermediates (*1*) for the synthesis of various fluorochemicals and fluoropolymers, such as fluorinated elastomers (*2*–*4*). However, the production of DIPFAs has been hampered by the lack of a method to obtain the compounds in high yield and purity. The tetrafluoroethylene telomerization reaction with iodine produces a mixture of DIPFAs, usually separated into its components by fractional distillation (*5*). The heavier DIPFAs cannot easily be separated with this method, thereby limiting the availability of α,ω-DIPFAs that are longer than eight carbon atoms.

Here, we report the application of supramolecular and crystal-engineering principles to the resolution of DIPFA mixtures through selective and reversible capture by ionic organic solids. We initially observed selective crystallization of a given DIPFA **2** from solutions of size-matched bis(trimethylammonium) alkane diiodides **1** (Scheme 1). Furthermore, we found that even microcrystalline powders of the iodide salts could selectively incorporate matched DIPFAs from the gas phase despite the absence of porosity in the static crystal structures. Thus, **1a** to **1f** represent a class of dynamically porous materials (*6*).

We have already demonstrated that DIPFAs behave as robust telechelic halogen-bonding (*7*, *8*) donors, given that fluorine inductively boosts the electron density acceptor ability of the terminal iodine substituents (*9*). For this reason, α,ω-DIPFAs form particularly strong halogen bonds when interacting with naked iodide ions (*10*) and result in trimeric supramolecular anions of the type $I^-\cdots I(CF_2)_mI\cdots I^-$ (*11*). Our goal was to incorporate this superion into a crystal framework that would achieve peak stability for a given-sized DIPFA (*12*). We reasoned that matching the size of this halogen-bonded superanion with a terminally functionalized dication of similar dimensions should increase the strength of electrostatic binding in an ionic lattice, thus driving a selective molecular recognition of the target DIPFA. We therefore selected the iodide salts of the bis(trimethylammonium) alkane derivatives **1a-f** (*13*), which are well-known structure-directing agents in zeolite synthesis (*14*) and guests in supramolecular chemistry (*15*).

Single-crystal x-ray analysis of **1b**·$2H_2O$ (Fig. 1A) (*16*) shows that water is hydrogen-bonded to iodide ions ($H\cdots I^-$ has distances of 2.766 to 2.804 Å) and also weakly interacts with the methyl and methylene H atoms of the cation.

[1]Laboratory of Nanostructured Fluorinated Materials, Department of Chemistry, Materials, and Chemical Engineering Giulio Natta, Politecnico di Milano, via L. Mancinelli 7, 20131 Milan, Italy. [2]Department of Chemistry, University of Jyväskylä, Post Office Box 35, Jyväskylä FI–40014, Finland. [3]Istituto di Scienze e Tecnologie Molecolari–Consiglio Nazionale delle Ricerche, University of Milan, 20133 Milan, Italy. [4]Nanoscience Center, Department of Chemistry, University of Jyväskylä, Post Office Box 35, Jyväskylä FI–40014, Finland. [5]Air Force Research Laboratory/RZSP, 10 East Saturn Boulevard, Edwards Air Force Base, CA 93524, USA.

*To whom correspondence should be addressed. E-mail: pierangelo.metrangolo@polimi.it.

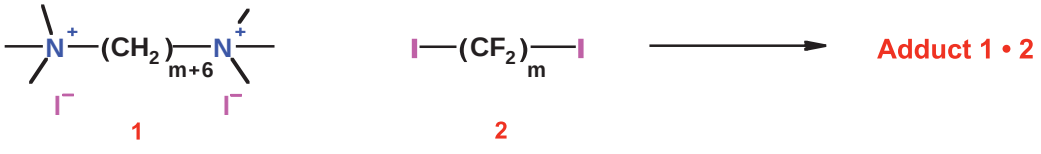

1, 2	a	b	c	d	e	f
m	2	4	6	8	10	12

Adduct	Distance A $^+N(CH_2)_{m+6}N^+$ (Å)	Distance B $I^-\cdots I(CF_2)_mI\cdots I^-$ (Å)		Δ (B - A) (Å)	Distance $I^-\cdots I$ (Å)	Angle $I^-\cdots I$-C (°)
1a • 2a	11.290(14)	12.056(5)	MATCH	0.766	3.478(2)	167.8(4)
1b • 2b	13.628(12)	14.483(4)	MATCH	0.855	3.4517(11)	166.0(4)
1c • 2c	16.395(11)	17.083(5)	MATCH	0.688	3.4627(11)	167.5(2)
1b • 2d	13.62(4)	18.797(4)	MISMATCH	5.177	3.357(3), 3.410(2)	173.3(7), 176.1(6)
1a • 2b	10.527(8)	14.104(3)	MISMATCH	3.577	3.3514(9)	174.7(4)

Scheme 1.

These interactions alongside the anion-cation interactions dominate the crystal structure. The bis(trimethylammonium) decane molecule adopts the usual all-trans conformation, and the hydrocarbon chains are parallel and interdigitated.

The N^+–N^+ intramolecular distance in crystalline **1b** of 13.965 Å is well-matched to the I^-–I^- distance in the $I^-\cdots I(CF_2)_4I\cdots I^-$ superanion, as found in our previous study (*17*). For this reason, we attempted to crystallize **1b** together with 1,4-diiodooctafluorobutane **2b**, starting from their equimolar CH_3OH and $CHCl_3$ solutions, respectively. Upon mixing of the two solutions, the 1:1 supramolecular complex **1b·2b** crystallized in a nearly quantitative yield and purity. Single-crystal x-ray analysis of the complex **1b·2b** confirmed our initial hypothesis: The distance between the intramolecular N atoms of **1b** in the complex is within 1 Å of the iodide ions' spacing in the superanion $I^-\cdots I(CF_2)_4I\cdots I^-$ ($\Delta = 0.855$ Å) (Scheme 1). Four alkyl dications define a rectangular parallelepiped-shaped cavity that encapsulates DIPFA **2b**, trapped by strong halogen bonds to the two I^- ions at either end (Fig. 1, B and C). As a probable consequence of the optimized binding that results from the structural complementarity of the interacting charged moieties and the matching sizes of the two starting compounds **1b** and **2b**, complex **1b·2b** shows a very low solubility in organic solvents as compared with that of pure starting materials. The $I^-\cdots$I-C distance of 3.452 Å, which is noticeably shorter than the sum of the van der Waals radius of the iodine atom and the Pauling radius for the I^- ion (4.14 Å) (*18*), indicates strong halogen bonding (*7*).

To test the generality of the size-matching hypothesis, we challenged salt **1a** with DIPFA **2a** and **1c** with **2c** (Scheme 1), maintaining the scaling relationship of **1b** and **2b**. Indeed, the complexes **1a·2a** (fig. S1) and **1c·2c** (Fig. 1D) both exhibit crystal lattices analogous to that of the **1b·2b** complex. In fact, two of the unit cell dimensions in each case are nearly the same (~6 and ~8 Å), indicating similar packing in those two directions, and the third dimension is related to the relative differences in the length of the molecules.

The importance of size matching was further confirmed by the isolation and structural characterization of two mismatched complexes, **1a·2b** and **1b·2d** (Scheme 1). In complex **1a·2b**, the discrete superanion $I^-\cdots I(CF_2)_4I\cdots I^-$ still forms ($I^-\cdots$I-C has a distance of 3.351 Å and angle of 174.70°), but the crystal packing is completely different from that in the matched structures. There is no cavity in which to trap the DIPFA; instead, the structure consists of cation and superanion layers (fig. S3). An even greater change occurs in the complex **1b·2d**, which crystallizes in a 1:2 stoichiometry and distributes the DIPFAs **2d** with alternating I^- ions in an infinite one-dimensional (1D) halogen-bonded polyanionic chain geometry ($I^-\cdots$I-C has distances of 3.357 and 3.410 Å and angles of 173.30 and 176.10°) (fig. S4).

All matched complexes (**1a·2a**, **1b·2b**, and **1c·2c**) show melting points higher than the mismatched ones in their respective homolog series, which is consistent with a higher stability of the crystal lattices with well-organized cavities around the DIPFAs. We therefore surmised that the enhanced stability should translate to a selective molecular recognition of a given DIPFA from a solution mixture by the size-matched salt **1** (*11*, *19*).

With this in mind, we performed competitive crystallization experiments by dissolving one equivalent of all four commercially available α,ω-DIPFAs **2a-d** into the same $CHCl_3$ solution. When this solution was added to a CH_3OH solution containing one equivalent of a single salt (from among **1a-d**), only the size-matched DIPFA was crystallized from the combined solution. Complexes at all four chain lengths (**a-d**) could be isolated in quantitative yield and purity. Although we were not able to obtain single-crystal x-ray data for the complex **1d·2d**, powder x-ray diffraction (PXRD) analysis confirmed the similarities in packing between **1d·2d** and the other matched complexes **1a-c·2a-c** (figs. S7 to S10). The above-described competitive crystallization experiment confirms the further generality of the size-matching rule for compounds $\mathbf{1}_{m+6}$ and $\mathbf{2}_m$. Once the matched DIPFA had been completely separated from the solution by filtering out the corresponding $\mathbf{1}_{m+6}\cdot\mathbf{2}_m$ solid adduct, the addition to the solution of another equivalent of the same chain-length salt **1** consistently afforded a white solid comprising a mixture of all the other possible **1·2** mismatched complexes that were present in varying mass fractions.

Intrigued by the isolation of the **1d·2d** complex, we extended the selective crystallization method to a mixture of higher DIPFA telomers that were found in a distillation residue obtained from industry with the following mass fraction composition: 1,8-diiodoperfluorooctane **2d** (24.2%), 1,10-diiodoperfluorodecane **2e** (41.9%), 1,12-diiodoperfluorododecane **2f** (23.0%), 1,14-diiodoperfluorotetradecane (8.3%), and 1,16-diiodoperfluorohexadecane (2.6%). The α,ω-DIPFA mixture was dissolved in CCl_4 and combined with a CH_3OH solution of bis(trimethylammonium) hexadecane diiodide **1e** (one equivalent of **1e** for one equivalent of **2e** in the mixture). A white solid precipitated almost immediately. Gas chromatography (GC)

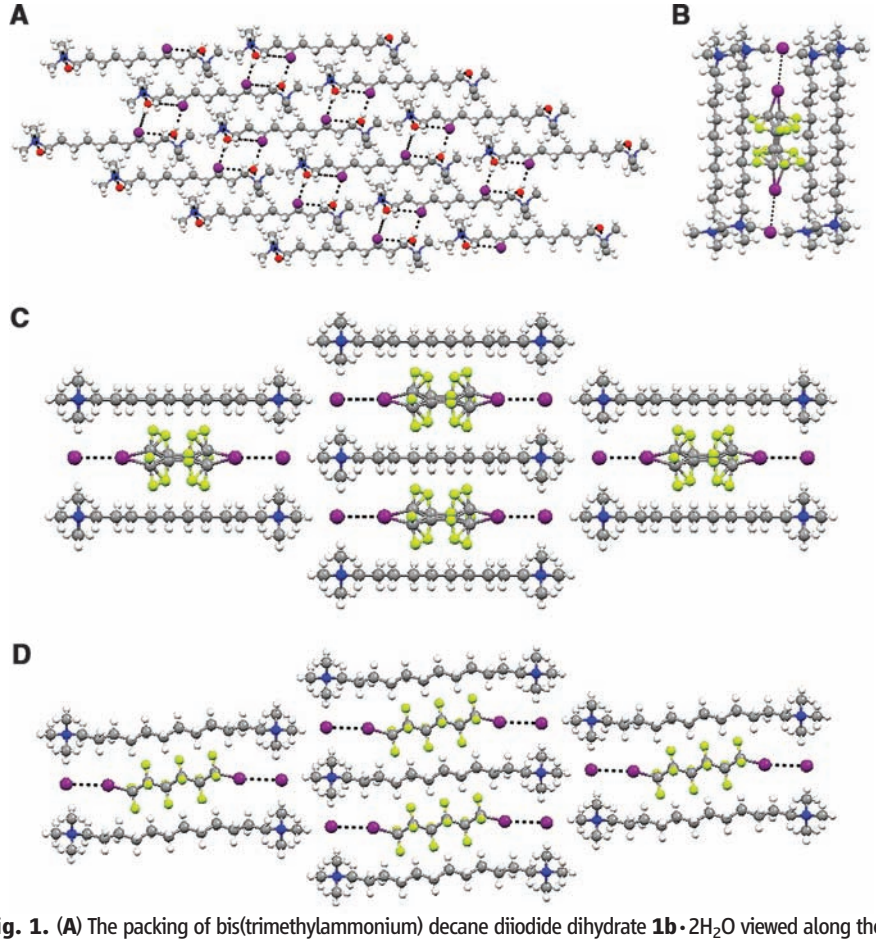

Fig. 1. (**A**) The packing of bis(trimethylammonium) decane diiodide dihydrate **1b**·$2H_2O$ viewed along the *a* axis. (**B**) The complex bis(trimethylammonium) decane diiodide/diiodoperfluorobutane **1b·2b**. Shown is a view of the molecular cavity defined by four alkyl dications, with encapsulated guest **2b** halogen-bonded to I^- ions at the top and bottom. (**C**) The crystal packing of the complex **1b·2b** viewed along the *c* axis. Both of the disordered orientations of **2b** are shown in (B) and (C). (**D**) The crystal packing of the complex **1c·2c** viewed along the *a* axis. The software package Mercury 1.4.2 (available for free download from www.ccdc.cam.ac.uk) was used to construct these images from the crystallographic information files. Gray, carbon; white, hydrogen; green, fluorine; blue, nitrogen; red, oxygen; magenta, iodine. Halogen bonds are depicted as dotted lines.

analysis indicated that **2e** was the only α,ω-DIPFA present in this solid. Nuclear magnetic resonance (NMR) experiments and melting point analysis on the solid confirmed the 1:1 ratio of the perfluorocarbon (PFC) and hydrocarbon (HC) components and thus the formation of the complex **1e·2e**. The same experiment was repeated by adding to a solution of the DIPFA mixture one equivalent of bis(trimethylammonium) octadecane diiodide **1f** in CH_3OH, which led to the rapid precipitation of the almost pure (>90%) 1,12-diiodoperfluorododecane complex **1f·2f** [based on GC, NMR, infrared (IR), and melting-point analysis] despite the low relative amount of **2f** in the starting mixture (23%).

Scattered examples in the open literature report the isolation of analytical samples of **2e** and **2f** by GC (*20*). Even in the vast patent literature on the preparation of α,ω-DIPFAs, we found no evidence of preparative and quantitative separation methods other than time- and energy-consuming fractional distillation, for which there was scarce indication of effectiveness in the purification of the higher telomers (*21*). Having thus characterized a selective crystallization technique with potentially great utility, we explored the reversibility of the binding of the DIPFAs in our matching complexes by means of various techniques. Our expectations were bolstered by the reversibility of halogen bonding and high DIPFA vapor pressure relative to salts **1**. Gas-phase IR spectra at ambient pressure in a sealed heated cell showed that the complex **1a·2a** starts to release **2a** at 433 K (the boiling point of pure **2a** is 385 K) with the maximum release occurring at 463 K, well before the melting temperature of the complex (474 K). Similar behavior was observed by use of thermogravimetric analysis (TGA) for the other **1b-d·2b-d** matched complexes (Table 1, figs. S19 to S30, and tables S8 to S10). In addition, PXRD, IR, melting-point, and NMR analyses confirmed that complete removal of **2a-d** yields the pure salts **1a-d** in the same crystal phases as the starting materials (figs. S15 to S18).

This robust liberation of the guest prompted us to study the reverse process, namely, the uptake of DIPFA vapors by the solid bis(trimethylammonium) alkane derivatives **1a-f**. Practical application of the selective molecular recognition would benefit from a nonsolvent environment. We placed finely ground ionic solids **1a**, **1b**, or **1c** in sealed nested jars so that they were isolated from surrounding liquid samples of the matched DIPFAs **2a**, **2b**, or **2c** but accessible to the corresponding vapor. The 1:1 matching complexes **1a·2a** and **1b·2b** were obtained after 6 hours and 7 days, respectively, at ambient pressure and temperature, and both complexes exhibited the same lattice structure observed from the solution crystallization (figs. S7 and S8). Because of the lower vapor pressure of **1c**, the 1:1 matching complex **1c·2c** required 3 days at 313 K to form fully; once again, the same crystal phase as from the solution was observed (Fig. 2, left). These gas-solid reactions thus transform a nonporous ionic solid into a well-ordered encapsulation complex.

The selectivity of these gas-solid reactions was further probed by the following guest-exchange reaction. The finely ground mismatched complex **1a·2b** was exposed to vapor of the matched DIPFA **2a** in a sealed vessel at ambient pressure and temperature for 7 days. PXRD data indicated that the mismatched DIPFA **2b** was completely replaced in this gas-solid reaction by the matched **2a**, yielding exclusively the 1:1 matching complex **1a·2a** in the same crystal form as had been obtained by means of solution crystallization (Fig. 2, D and E). The same experiment carried out on the matching complex **1a·2a** by means of exposure to vapor of the mismatched DIPFA **2b** did not result in any reaction (Fig. 2, F and G).

Nanoporous solids that are able to absorb and release small molecules in a controllable and selective fashion are rare but known in the literature (*22–26*). An alternative to nanoporosity is the controlled uptake and release of small molecules by means of reversible heterogeneous gas-solid reactions (*27–29*). In the present case of nonporous solid compounds, bis(trimethylammonium) alkane diiodides **1a-f** show a size-matching–based dynamic response upon exposure to gaseous α,ω-DIPFAs

Table 1. Observed and calculated weight losses for DIPFA removal from matching complexes **1a-d·2a-d**. Δwt_{obs}, observed weight loss for leaving compound; Δwt_{calc}, theoretical weight loss for leaving DIPFA; T_{end}, observed end temperature of DIPFA removal; T_m, melting point of the starting complex; β, heating rate.

Complex	Formula weight (g/mol)	Δwt_{obs} (%)	Δwt_{calc} (%)	T_{end} (K)	T_m (K)	β (K/min)
1a·2a	838.05	37.7	42.22 (**2a**)	464	474	10
1a·2a*		41.7	42.22 (**2a**)	463	474	10/isotherm
1b·2b	966.12	47.0	46.97 (**2b**)	493	503	10
1b·2b*		44.6	46.97 (**2b**)	463	503	10/isotherm
1c·2c	1094.20	50.5	50.62 (**2c**)	468	500	2
1c·2c*		49.8	50.62 (**2c**)	463	500	10/isotherm
1d·2d	1222.28	53.1	53.47 (**2d**)	486	504	2
1d·2d†		52.4	53.47 (**2d**)	486	504	10/isotherm

*Thermogravimetric run included an isothermal step at 463 K for 60 min. †Thermogravimetric run included an isothermal step at 448 K for 60 min.

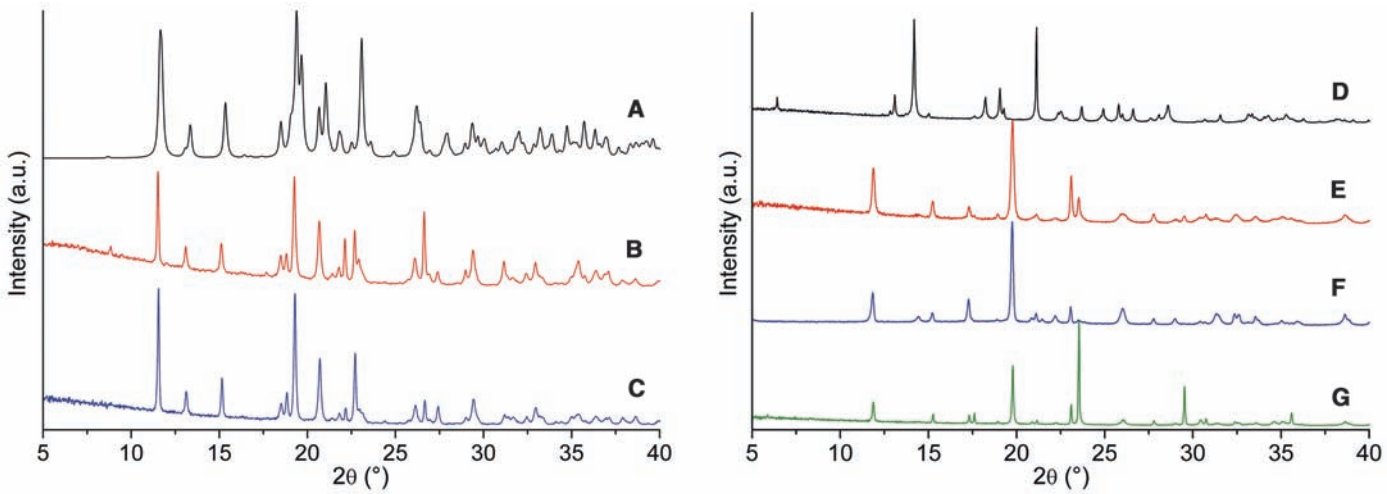

Fig. 2. (Left) PXRD patterns of the complex **1c·2c** (**A**) simulated from single-crystal x-ray data, (**B**) acquired after solution crystallization, and (**C**) acquired after gas-solid reaction. (Right) PXRD patterns of the mismatched complex **1a·2b** obtained from solution crystallization (**D**) before and (**E**) after exposure to vapor of 1,2-diiodoperfluoroethane **2a**. Below these are PXRD patterns of the matched complex **1a·2a** obtained from solution crystallization (**F**) before and (**G**) after exposure to vapor of 1,4-diiodoperfluorobutane **2b**.

2a-f, yielding the homologous series of supramolecular complexes $\mathbf{1}_{m+6}\cdot\mathbf{2}_m$. In such complexes, the complementarity of size leads to a structure type that overrides the strong driving force of PFC-HC segregation. This process is expected to require surmounting a considerable energy barrier, especially in the case of the very long DIPFA **2c**. Although the size-matching leads to one product, the PFC-HC segregation does not distinguish between various sizes of PFC and HC segments, as was proven by the observation of a variety of complexes produced from a size-mismatched PFC-HC mixture. Despite a lack of porosity of the starting materials **1a-f**, the DIPFAs **2a-f** are readily transported through the solid until a thermodynamically stable porous structure is achieved. A comparison with the x-ray structure of the pure salt **1b** (Fig. 1A) suggests that once the size-matching DIPFA forms halogen bonds with the I^- ions, the $I^-\cdots I(CF_2)_mI\cdots I^-$ superanion acts as a template of the porous structure observed by promoting the positional and/or orientational rearrangement of the hydrocarbon dications (analogously to the sliding filament model, such as what occurs between thick and thin filaments in myofibrils). Our results show the relevance of a supramolecular-templated assembly of dynamically porous materials.

Gas-solid reactions often entail profound transformations of the chemical and physical nature of the solid materials and rarely are of practical use. In the present case, the full reversibility of the process, whereby DIPFAs can first be selectively complexed and then quantitatively evacuated, yields purified fluorinated telomers and a reusable ionic scaffold. Beyond the practical potential for separating mixtures of α,ω-DIPFAs, we envision the application of this purification method to another vast class of compounds of industrial interest, the α,ω-diiodoperfluoropolyethers (DIPFPEs), which are useful intermediates for the synthesis of fluorocontaining resins, elastomers, and surfactants.

References and Notes

1. N. O. Brace, *J. Fluor. Chem.* **108**, 147 (2001).
2. B. Ameduri, B. Boutevin, *Well-Architectured Fluropolymers: Synthesis, Properties and Applications* (Elsevier, Amsterdam, 2004).
3. K. Baum, T. G. Archibald, A. A. Malik, *J. Org. Chem.* **59**, 6804 (1994).
4. A. L. Logothetis, in *Organofluorine Chemistry*, R. E. Banks, B. E. Smart, J. C. Tatlow, Eds. (Plenum, New York, 1994), pp. 373–396.
5. H.-P. Cao, Q.-Y. Chen, *J. Fluor. Chem.* **128**, 1187 (2007).
6. S. J. Dalgarno, P. K. Thallapally, L. J. Barbour, J. L. Atwood, *Chem. Soc. Rev.* **36**, 236 (2007).
7. P. Metrangolo, G. Resnati, *Chem. Eur. J.* **7**, 2511 (2001).
8. K. Rissanen, *CrystEngComm* **10**, 1107 (2008).
9. P. Metrangolo, G. Resnati, *Science* **321**, 918 (2008).
10. P. Metrangolo, H. Neukirch, T. Pilati, G. Resnati, *Acc. Chem. Res.* **38**, 386 (2005).
11. P. Metrangolo, F. Meyer, T. Pilati, G. Resnati, G. Terraneo, *Angew. Chem. Int. Ed.* **47**, 6114 (2008).
12. M. I. Nelen, A. V. Eliseev, *J. Chem. Soc. Perkin Trans. 2* 1359 (1997).
13. H.-G. Löhr *et al.*, *J. Org. Chem.* **49**, 1621 (1984).
14. P. Sun, Q. Jin, L. Wang, B. Li, D. Ding, *J. Porous Mater.* **10**, 145 (2003).
15. E. Menozzi, J. Rebek, *Chem. Commun. (Camb.)* **44**, 5530 (2005).
16. Materials and methods are available as supporting material on *Science* Online.
17. R. Liantonio, P. Metrangolo, T. Pilati, G. Resnati, *Cryst. Growth Des.* **3**, 355 (2003).
18. A. Bondi, *J. Phys. Chem.* **68**, 441 (1964).
19. M. W. Hosseini, J. M. Lehn, *J. Am. Chem. Soc.* **104**, 3525 (1982).
20. S. Boneva, St. Kotov, *Chromatographia* **25**, 735 (1988).
21. H. Dindi, J. J. Hagedorn, M.-H. Hung, U.S. Patent 6825389 (2004).
22. J. L. Atwood, L. J. Barbour, A. Jerga, B. L. Schottel, *Science* **298**, 1000 (2002).
23. P. K. Thallapally *et al.*, *Nat. Mater.* **7**, 146 (2008).
24. B. D. Chandler *et al.*, *Nat. Mater.* **7**, 229 (2008).
25. J. L. Atwood, L. J. Barbour, A. Jerga, *Science* **296**, 2367 (2002).
26. S. Kitagawa, K. Uemura, *Chem. Soc. Rev.* **34**, 109 (2005).
27. D. Braga *et al.*, *Angew. Chem. Int. Ed.* **45**, 142 (2006).
28. J. J. Vittal, *Coord. Chem. Rev.* **251**, 1781 (2007).
29. S. Libri *et al.*, *Angew. Chem. Int. Ed.* **47**, 1693 (2008).

30. P.M., T.P., and G.R. thank Fondazione Cariplo (Project "Self-Assembled Nanostructured Materials: A Strategy for the Control of Electrooptic Properties") for generous support. K.R. thanks the Academy of Finland (project 212588) for generous support. A.V. thanks the U.S. Air Force Research Laboratory/Air Force Office of Scientific Research for a generous Window on Europe grant, A. Garscadden for his endorsement, and R. Channell, R. Corley, and M. Huggins for their support. The authors declare no conflict of interest. A part of the present work is the object of the patent application PCT/EP2008/058588 (2008), priority date 7 November 2007, by Y.C., P.M., and G.R. to Politecnico di Milano. The authors' contributions were as follows: A.V., Y.C., M.L., T.P., and P.M. performed experiments; P.M., G.R., K.R., M.L., T.P., and Y.C. performed data analysis; and P.M., G.R., K.R., M.L., and T.P. wrote the paper. Crystallographic data for compounds **1a**•**2a**, **1a**•**2b**, **1b**•**2b**, **1b**•**2d**, **1b**, and **1c**•**2c** can be obtained free of charge from the Cambridge Crystallographic Data Centre via www.ccdc.cam.ac.uk/data_request/cif under reference numbers CCDC 709470 to 709475, respectively.

Supporting Online Material

www.sciencemag.org/cgi/content/full/323/5920/1461/DC1
Materials and Methods
Figs. S1 to S30
Tables S1 to S10
Schemes S1 to S2
References

18 November 2008; accepted 22 January 2009
10.1126/science.1168679

Time-Resolved Molecular Frame Dynamics of Fixed-in-Space CS_2 Molecules

Christer Z. Bisgaard,[1] Owen J. Clarkin,[1,2] Guorong Wu,[1] Anthony M. D. Lee,[1,2]* Oliver Geßner,[3] Carl C. Hayden,[4] Albert Stolow[1,2]†

Random orientation of molecules within a sample leads to blurred observations of chemical reactions studied from the laboratory perspective. Methods developed for the dynamic imaging of molecular structures and processes struggle with this, as measurements are optimally made in the molecular frame. We used laser alignment to transiently fix carbon disulfide molecules in space long enough to elucidate, in the molecular reference frame, details of ultrafast electronic-vibrational dynamics during a photochemical reaction. These three-dimensional photoelectron imaging results, combined with ongoing efforts in molecular alignment and orientation, presage a wide range of insights obtainable from time-resolved studies in the molecular frame.

Most molecules are non-spherical and so exhibit a dependence on their relative orientation in interactions with other molecules or with light. Measurements, therefore, should ideally be made in the molecular reference frame (MF). Unfortunately, in the gas and liquid phases, molecules are generally randomly oriented in the laboratory frame (LF) to which most standard techniques are referenced, leading to blurred observations of molecular properties and processes. An analogy is the difference between single-crystal versus powder x-ray diffraction, the former revealing the greatest details of molecular structure. Other examples include the determination of vector correlations in photodissociation dynamics (*1*) and measurements of (time-independent) photoelectron angular distributions (PADs) of fixed-in-space molecules, which has been a goal of researchers since the 1970s (*2*) and was achieved for selected cases (*3*, *4*). Promising ultrafast techniques for imaging structural and electronic changes during molecular processes, such as time-resolved x-ray (*5*) and electron (*6*, *7*) diffraction, tomographic orbital imaging (*8*), time-resolved photoelectron spectroscopy (TRPES) (*9*, *10*), laser-induced electron diffraction (*11*), and high harmonic generation (*12*), would all benefit from avoidance of this

[1]Steacie Institute for Molecular Sciences, National Research Council Canada, 100 Sussex Drive, Ottawa, Ontario K1A 0R6, Canada. [2]Department of Chemistry, Queen's University, Kingston, Ontario K7L 3N6, Canada. [3]Chemical Sciences Division, Lawrence Berkeley National Laboratory, One Cyclotron Road, M/S 2-300, Berkeley, CA 94720, USA. [4]Combustion Research Facility, Sandia National Laboratory, Livermore, CA 94551, USA.

*Present address: Department of Cancer Imaging, BC Cancer Research Centre, Vancouver, British Columbia V5Z 1L3, Canada.

†To whom correspondence should be addressed. E-mail: albert.stolow@nrc.ca